

Manganese–Tyrosine Interaction in the Photosystem II Oxygen-Evolving Complex

Xiao-Song Tang,*[§] David W. Randall,[†] Dee Ann Force,[†]
Bruce A. Diner,*[§] and R. David Britt*[†]

Department of Chemistry, University of California
Davis, California 95616-0935

E. I. du Pont de Nemours & Company Central Research and
Development Department, Wilmington, Delaware 19880-0173

Received April 1, 1996

Photosystem II (PS II) carries out the photochemical extraction of electrons from water, forming molecular oxygen in the process. The catalytic center for this essential four-electron oxidation reaction is known as the oxygen-evolving complex (OEC). A broad radical electron paramagnetic resonance (EPR) signal can be photogenerated in photosystem II following a variety of treatments that inhibit oxygen evolution.^{1–5} The radical has line widths between 90 and 240 G (full width at half-maximum) depending on the specific treatment, and has a characteristic “split” line shape (Figure 1A). The molecular origin of this signal has been intensely debated,^{6,7} with possibilities including oxidized histidine,^{8–10} partially oxidized substrate water,¹¹ or the redox-active tyrosine, Y_Z, that is the sole electron transfer intermediate between the photooxidized P₆₈₀⁺ chlorophyll moiety and the tetranuclear Mn cluster at the heart of the OEC.^{4,12,13} The species giving rise to the split EPR signal is in close proximity (approximately 4.5 Å¹²) to the Mn cluster, which accounts for its broad line width.^{8,12} We report the results of continuous wave and pulsed EPR experiments performed on this signal in photosystem II particles in which tyrosine is specifically labeled with deuterons in the nonexchangeable hydrogen positions. These experiments conclusively demonstrate that the split EPR signal originates from tyrosine and provide strong support for new metalloradical mechanistic models for oxygen evolution invoking tyrosine Y_Z in proton^{7,12,14} or hydrogen atom^{15,16} abstraction from substrate water bound to the Mn cluster of the OEC.

Cells of *Synechocystis* PCC 6803 were grown photoautotrophically on either deuterated tyrosine (*d*₇-Tyr) or natural

abundance tyrosine (*h*₇-Tyr).¹⁷ Oxygen-evolving PS II core complexes¹⁸ were washed with pH 5.5 acetate buffer⁵ (40 mM Mes-NaOH, 500 mM acetate, and 300 mM sucrose) and then centrifuged (266000g, 1 h) in the presence of 8% polyethylene glycol (final concentration).¹⁹ The complexes were resuspended in the acetate buffer, the chlorophyll concentration was adjusted to 2–3 mg/mL, and 0.3 mM potassium ferricyanide (final concentration) was added. The acetate-treated PS II samples were frozen during illumination²⁰ in order to generate the split-signal radical. The radical was later eliminated for baseline subtraction purposes by dark annealing the sample at 0 °C for 30 min. CW-EPR spectra were recorded on a Bruker ER200D spectrometer. Electron-spin echo envelope modulation (ESEEM) experiments were performed with a 1 kW pulsed EPR spectrometer.²¹ Three-pulse ESEEM experiments were performed by incrementing the time *T* in the stimulated echo sequence: $\pi/2-\tau-\pi/2-T-\pi/2-\tau$ —stimulated echo.²²

Previously, a split EPR signal in *Synechocystis* PS II particles has been reported following Ca²⁺-depletion.²⁴ However, the 40 G wide signal from tyrosine Y_D^{*} (as measured under pulsed EPR field swept conditions) overlaps significantly with this weak 90 G wide signal, making it difficult to perform high-resolution ENDOR or ESEEM experiments on the split EPR signal. The acetate treatment used here produces a more intense and broader split EPR signal in *Synechocystis* PS II core complexes. Figure 1B shows an expanded CW-EPR spectrum of the acetate-generated split EPR signal, which has a line width of approximately 220 G. The insert of Figure 1B shows a detailed view of the dark-stable tyrosine Y_D^{*} EPR signal,¹⁷ and the dramatic line shape difference between deuterated (trace b) and control (trace a) samples demonstrates that deuterated tyrosine is indeed incorporated into the PS II proteins. Examination of the data in Figure 1B shows that the line width of the split EPR signal observed in the *d*₇-Tyr labeled PS II core complexes (dashed line) is slightly narrower (by ~10 G) than that in *h*₇-Tyr natural abundance PS II core complexes (solid line). The observation of only a small isotopic narrowing is not surprising since the width of the split signal is dominated by the electron spin–electron spin interaction. Nevertheless, this result suggests that tyrosine is the origin of the split EPR signal, though EPR alone does not provide sufficient sensitivity to the isotopic substitution to make a conclusive assignment.

ESEEM spectroscopy combined with selective isotopic substitution can provide definitive molecular assignments.²⁵ Figure 2 shows the results of three-pulse ESEEM experiments on the acetate-treated *Synechocystis* samples. Panel A shows frequency domain ESEEM spectra ($\tau = 189$ ns) of Y_D^{*} in samples with natural abundance vs deuterated tyrosine. Also shown (bold line) is a ratioed ²H/¹H spectrum which eliminates contributions from other nuclei: only tyrosine deuterons or

(17) Barry, B. A.; Babcock, G. T. *Proc. Natl. Acad. Sci. U.S.A.* **1987**, *84*, 7099–7103.

(18) Tang, X.-S.; Diner, B. A. *Biochemistry* **1994**, *33*, 4594–4603.

(19) The acetate treatment used here is similar to that of Maclachlan and Nugent⁵ up to the final dialysis against 10 mM acetate (pH 5.5, 300 mM sucrose, 40 mM Mes) which was not performed; the buffer for the samples in the EPR tubes was the 500 mM acetate buffer described in the text. Eliminating this dialysis procedure increased the intensity of the split EPR signal in *Synechocystis*.

(20) Tang, X.-S.; Zheng, M.; Chisholm, D. A.; Dismukes, G. C.; Diner, B. A. *Biochemistry* **1996**, *35*, 1475–1484.

(21) Sturgeon, B. E.; Britt, R. D. *Rev. Sci. Instrum.* **1992**, *63*, 2187–2192.

(22) Britt, R. D. In *Biophysical Techniques in Photosynthesis*; Amesz, J., Hoff, A. J., Eds.; Kluwer Academic: Dordrecht, The Netherlands, 1996; pp 235–253.

(23) Mims, W. B. *J. Magn. Reson.* **1984**, *59*, 291–306.

(24) Kirilovsky, D. L.; Boussac, A. G. P.; van Mieghem, F. J. E.; Ducruet, J.-M. R. C.; Sétif, P. R.; Yu, J.; Vermaas, W. F. J.; Rutherford, A. W. *Biochemistry* **1992**, *31*, 2099–2107.

(25) Tang, X.-S.; Diner, B. A.; Larsen, B. S.; Gilchrist, M. L.; Lorigan, G. A.; Britt, R. D. *Proc. Natl. Acad. Sci. U.S.A.* **1994**, *91*, 704–708.

[§] E. I. du Pont de Nemours & Co.

[†] University of California.

(1) Boussac, A.; Zimmermann, J.-L.; Rutherford, A. W. *Biochemistry* **1989**, *28*, 8984–8989.

(2) Baumgarten, M.; Philo, J. S.; Dismukes, G. C. *Biochemistry* **1990**, *29*, 10814–10822.

(3) Boussac, A. P.; Setif, P.; Rutherford, A. W. *Biochemistry* **1992**, *31*, 1224–1234.

(4) Hallahan, B. J.; Nugent, J. H. A.; Warden, J. T.; Evans, M. C. W. *Biochemistry* **1992**, *31*, 4562–4573.

(5) Maclachlan, D. J.; Nugent, J. H. A. *Biochemistry* **1993**, *32*, 9772–9780.

(6) Debus, R. J. *Biochim. Biophys. Acta* **1992**, *1102*, 269–352.

(7) Britt, R. D. In *Oxygenic Photosynthesis: The Light Reactions*; Ort, D. R., Yocum, C. F., Eds.; Kluwer Academic: Dordrecht, The Netherlands, 1996; pp 137–164.

(8) Boussac, A.; Zimmermann, J.-L.; Rutherford, A. W.; Lavergne, J. *Nature* **1990**, *347*, 303–306.

(9) Berthomieu, C.; Boussac, A. *Biochemistry* **1995**, *34*, 1541–1548.

(10) Boussac, A.; Rutherford, A. W. *Biochemistry* **1992**, *31*, 7441–7445.

(11) Kusunoki, M. *Chem. Phys. Lett.* **1995**, *239*, 148–157.

(12) Gilchrist, M. L.; Ball, J. A.; Randall, D. W.; Britt, R. D. *Proc. Natl. Acad. Sci. U.S.A.* **1995**, *92*, 9545–9549.

(13) Britt, R. D.; Randall, D. W.; Ball, J. A.; Gilchrist, M. L., Jr.; Force, D. A.; Sturgeon, B. E.; Lorigan, G. A.; Tang, X.-S.; Diner, B. A.; Klein, M. P.; Chan, M. K.; Armstrong, W. H. In *Photosynthesis: from Light to Biosphere*; Mathis, P., Ed.; Kluwer Academic Publishers: Dordrecht, The Netherlands, 1995; pp 223–228.

(14) Force, D. A.; Randall, D. W.; Britt, R. D.; Tang, X.-S.; Diner, B. A. *J. Am. Chem. Soc.* **1995**, *117*, 12643–12644.

(15) Hoganson, C. W.; Lyadkis-Simantiris, N.; Tang, X.-S.; Tommos, C.; Warncke, K.; Babcock, G. T.; Diner, B. A.; McCracken, J.; Styring, S. *Photosyn. Res.* **1995**, *46*, 177–184.

(16) Tommos, C.; Tang, X.-S.; Warncke, K.; Hoganson, C. W.; Styring, S.; McCracken, J.; Diner, B. A.; Babcock, G. T. *J. Am. Chem. Soc.* **1995**, *117*, 10325–10335.

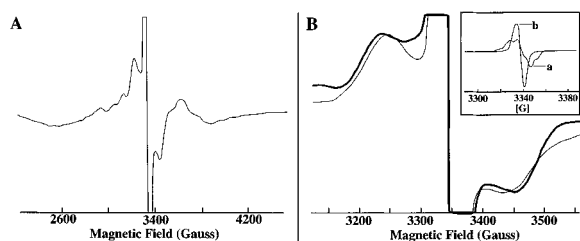


Figure 1. (A) The illuminated-minus-dark split EPR signal obtained from acetate-treated *Synechocystis* PS II core complexes. (B) Split EPR signal spectra of *Synechocystis* PS II core complexes isolated from cells containing h_7 -Tyr (thick line) or d_7 -Tyr (thin line). The inset shows the EPR signal of the dark-stable Y_D^{\bullet} radical in PS II core complexes containing h_7 -Tyr (a) or d_7 -Tyr (b). Instrument settings: microwave frequency, 9.371 (A), 9.385 GHz (B), 9.367 GHz (inset); microwave power, 32 mW (A); 2 mW (B), 0.1 mW (inset); modulation amplitude, 20 G (A and B), 2 G (inset); modulation frequency, 100 kHz; temperature, 10 K (A and B), 150 K (inset).

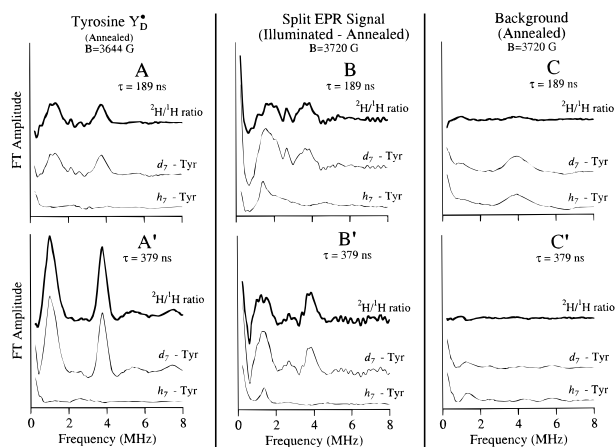
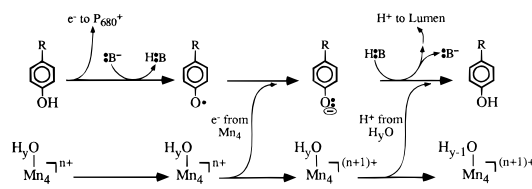


Figure 2. Normalized three-pulse ESEEM Frequency domain spectra²³ (FFT axis in arbitrary units) obtained from acetate-treated *Synechocystis* PS II core complexes. The traces have been offset for clarity. (A) Annealed Y_D^{\bullet} radical: ($^2\text{H}/^1\text{H}$) ratio (bold trace), d_7 -Tyr (middle trace), and h_7 -Tyr (lowest trace); $\tau = 189$ ns. (B) Illuminated-minus-annealed split-signal radical: ($^2\text{H}/^1\text{H}$) ratio (bold trace), d_7 -Tyr (middle trace), and h_7 -Tyr (lowest trace); $\tau = 189$ ns. (C) Background (annealed): ($^2\text{H}/^1\text{H}$) ratio (bold trace), d_7 -Tyr (middle trace), and h_7 -Tyr (lowest trace); $\tau = 189$ ns. (A', B', C'): As in (A),(B),(C) except $\tau = 379$ ns. Instrumental conditions: microwave frequency, 10.199 GHz; microwave power, 40 W; microwave $\pi/2$ pulse width, 15 ns; magnetic field, 3720 G (split EPR signal), 3644 G (Y_D^{\bullet}); repetition rate, 1 kHz (split EPR signal), 200 Hz (Y_D^{\bullet}); temperature, 4.2 K.

protons contribute to the ratioed spectra.²⁶ The ^2H ESEEM spectrum of Y_D^{\bullet} consists of features at 1.0 and 3.8 MHz from a strongly coupled β -methylene deuteron and deuterons at the 3 and 5 positions of the phenyl ring.²⁷ The weaker transitions at 2.1 and 2.6 MHz are due to a more weakly coupled β -methylene deuteron and deuterons at the 2 and 6 positions.²⁷ Panel B shows ESEEM spectra for the light-minus-annealed split EPR signal, and panel C shows the ESEEM spectra for the background signal of the annealed samples obtained at the same magnetic field value. The spectra of the split EPR signal are obtained by subtracting the time-domain modulation patterns of the annealed sample from those of the illuminated samples and then performing the Fourier analysis. The differences between the ESEEM spectra of the light-minus-annealed split EPR signal with d_7 -Tyr and h_7 -Tyr are unmistakable (panel B), while the background annealed traces are virtually identical (panel C) in spite of the different isotope labels. The clear difference

Scheme 1



between ESEEM spectra observed on the isotopically inequivalent samples is **conclusive** evidence that the split EPR signal originates from a tyrosyl radical. The striking similarity between the ratioed spectra of Y_D^{\bullet} (panel A) and the split-signal radical (panel B) is consistent with this assignment. The ESEEM spectrum of the split EPR signal is also quite similar to that of deuterated Y_Z^{\bullet} cryotrapped following illumination of Mn-depleted PS II lacking Y_D .¹⁶ The ESEEM spectral features of the split EPR signal are assigned in analogy with those of Y_D^{\bullet} ²⁷ and Y_Z^{\bullet} .¹⁶ Because τ -dependent peak suppressions occur in three-pulse ESEEM spectra it is useful to perform experiments at different τ values. Thus, the results of experiments performed at $\tau = 379$ ns are presented in panels A', B', and C'.

These selectively labeled tyrosine ESEEM results conclusively prove that the split EPR signal arises from a photogenerated tyrosine radical. Given that the Y_Z^{\bullet} tyrosine radical is photogenerated in functional PS II, it is almost certain that it is the Y_Z^{\bullet} tyrosine observed here as the split EPR signal. The Y_Z^{\bullet} rereduction kinetics can be slowed by treatments that inhibit oxygen evolution,²⁸ and this allows a fraction of the Y_Z^{\bullet} radical to be cryotrapped during illumination. The breadth of the split EPR signal results from the close proximity of the Mn cluster (ca. 4.5 Å).¹² This close proximity serves as the basis for new mechanistic models invoking Y_Z^{\bullet} directly in water oxidation.^{7,12,15,16} Scheme 1 presents an electron-mediated proton transfer mechanism by which Y_Z^{\bullet} could abstract protons from substrate water molecules acidified by binding to the high-valence Mn cluster. The scheme starts with the oxidation of Y_Z by photo-generated P_{680}^+ . It is known that the resulting tyrosine radical is neutral,²⁹ and following oxidation of Y_Z , the phenolic proton could be transported to the luminal phase via some intermediary basic residue(s) (B in this scheme). The manganese cluster is then oxidized by the tyrosyl radical, resulting in the formation of a strongly basic tyrosinate species. The tyrosinate base then abstracts a proton from water bound to the Mn cluster. Alternatively, advancement from the neutral tyrosyl radical to the tyrosine with an oxidized cluster could also be accomplished by a single hydrogen atom transfer.^{7,15} These proton or H atom abstractions depicted in Scheme 1 may occur in all S-state³⁰ transitions or in some subset thereof, for example, only the final $S_3 \rightarrow S_4$ transition which leads to the release of O_2 . This work, demonstrating that the split EPR signal arises from tyrosine Y_Z^{\bullet} in close proximity to the Mn cluster, indicates that mechanistic models for photosynthetic water oxidation need to include the possibility of such concerted tyrosine radical–Mn cluster interactions.

Acknowledgment. We acknowledge valuable advice from Gary Brudvig regarding the preparation of acetate-inhibited samples. A grant from the N.I.H. to R.D.B. and NRICGP grants from the U.S.D.A. to R.D.B. and B.A.D. are acknowledged. This work was partially supported by the Central R&D Department of E. I. du Pont de Nemours & Co. and is Contribution No. 7392.

JA9610592

(28) Andréasson, L.-E.; Lindberg, K. *Biochim. Biophys. Acta* **1992**, *1100*, 177–183.

(29) Babcock, G. T.; Barry, B. A.; Debus, R. J.; Hoganson, C. W.; Atamian, M.; McIntosh, L.; Sithole, I.; Yocum, C. F. *Biochemistry* **1989**, *28*, 9557–9565.

(30) Kok, B.; Forbush, B.; McGloin, M. *Photochem. Photobiol.* **1970**, *11*, 457–475.

(26) Mims, W. B.; Davis, J. L.; Peisach, J. *J. Magn. Reson.* **1990**, *86*, 273–292.

(27) Warncke, K.; Babcock, G. T.; McCracken, J. *J. Am. Chem. Soc.* **1994**, *116*, 7332–7340.